4ICEGE Thessaloniki-GREECE 2007

4th International Conference on
Earthquake Geotechnical Engineering
June 25-28, 2007
Paper No. 1640

ANALYTICAL VERIFICATION OF BURIED STEEL PIPELINES AT STRIKE-SLIP FAULT CROSSINGS

Dimitrios KARAMITROS[1], George BOUCKOVALAS[2], and George KOURETZIS[3]

ABSTRACT

Existing analytical methods for the stress analysis of buried steel pipelines at crossings with active strike-slip faults depend on a number of simplifications, which limit their applicability and may even lead to non-conservative results. The analytical methodology presented herein maintains the well-established assumptions of existing methodologies, but also introduces a number of refinements in order to achieve a more wide range of application without any major simplicity sacrifice. More specifically, it employs equations of equilibrium and compatibility of displacements to derive the axial force applied on the pipeline and adopts a combination of beam-on-elastic-foundation and elastic-beam theory to calculate the developing bending moment. Although indirectly, material and large-displacement non-linearities are also taken into account, while the actual distribution of stresses on the pipeline cross-section is considered for the calculation of the maximum design strain.

Keywords: buried steel pipelines, strike-slip faults, stress analysis, design

INTRODUCTION

Evaluation of the response of buried steel pipelines at active fault crossings is among their top seismic design priorities. This is because the axial and bending strains induced to the pipeline by step-like permanent ground deformation may become fairly large and lead to rupture, either due to tension or due to buckling. Apart from the detrimental effects that such a rupture can have to the operation of critical lifeline systems (EERI, 1999, Uzarski and Arnold, 2001), an irrecoverable ecological disaster may also result from the leakage of environmentally hazardous materials such as natural gas, fuel or liquid waste.

A simplified methodology which is widely used today for strike-slip and normal faults, is the one originally proposed by Kennedy et al. (1977), and consequently adopted by the ASCE (1984) guidelines for the seismic design of pipelines. Kennedy et al. extended the pioneering work of Newmark & Hall (1975), by taking into account soil-pipeline interaction in the transverse, as well as in the longitudinal direction. Their methodology applies to cases where the fault rupture provokes severe elongation of the pipeline, so as tension is the prevailing mode of deformation.

Wang & Yeh (1985) tried to overcome this shortcoming by taking the pipeline bending stiffness into account. Their methodology refers only to strike-slip faults and relies on partitioning of the pipeline into four (4) distinct segments: two (2) in the high curvature zone on both sides of the fault trace, and another two (2) outside this zone. The latter segments are treated as beams-on-elastic-foundation,

[1] Department of Geotechnical Engineering, School of Civil Engineering, National Technical University of Athens, Greece, Email: dimkaram@central.ntua.gr
[2] Professor, Department of Geotechnical Engineering, School of Civil Engineering, National Technical University of Athens, Greece, Email
[3] Department of Geotechnical Engineering, School of Civil Engineering, National Technical University of Athens, Greece

while the former ones are assumed to deform as circular arcs, with a radius of curvature calculated from the equations of equilibrium and the demand for continuity between adjacent segments. Although clearly advanced, compared to the methodology of Kennedy et al. (1977), the methodology of Wang and Yeh also features two main pitfalls, which may lead to non-conservative predictions: (a) the most unfavorable combination of axial and bending strains along the pipeline is assumed to develop outside the high-curvature zone and (b) the effect of axial tension on the pipeline's bending stiffness is overlooked.

METHODOLOGY OUTLINE

In summary, the proposed methodology computes axial and bending strains along the pipeline with the aid of beam-on-elastic-foundation and elastic-beam theories, taking into account the bending stiffness of the pipeline cross-section, as well as the soil-pipeline interaction effects in both the axial and the transverse directions. Material non-linearity is considered by assuming a bilinear stress-strain relationship for the pipeline steel, combined with an iterative linear elastic solution scheme which uses the secant Young's modulus of the pipeline steel in order to ensure compatibility between computed non-linear stresses and strains.

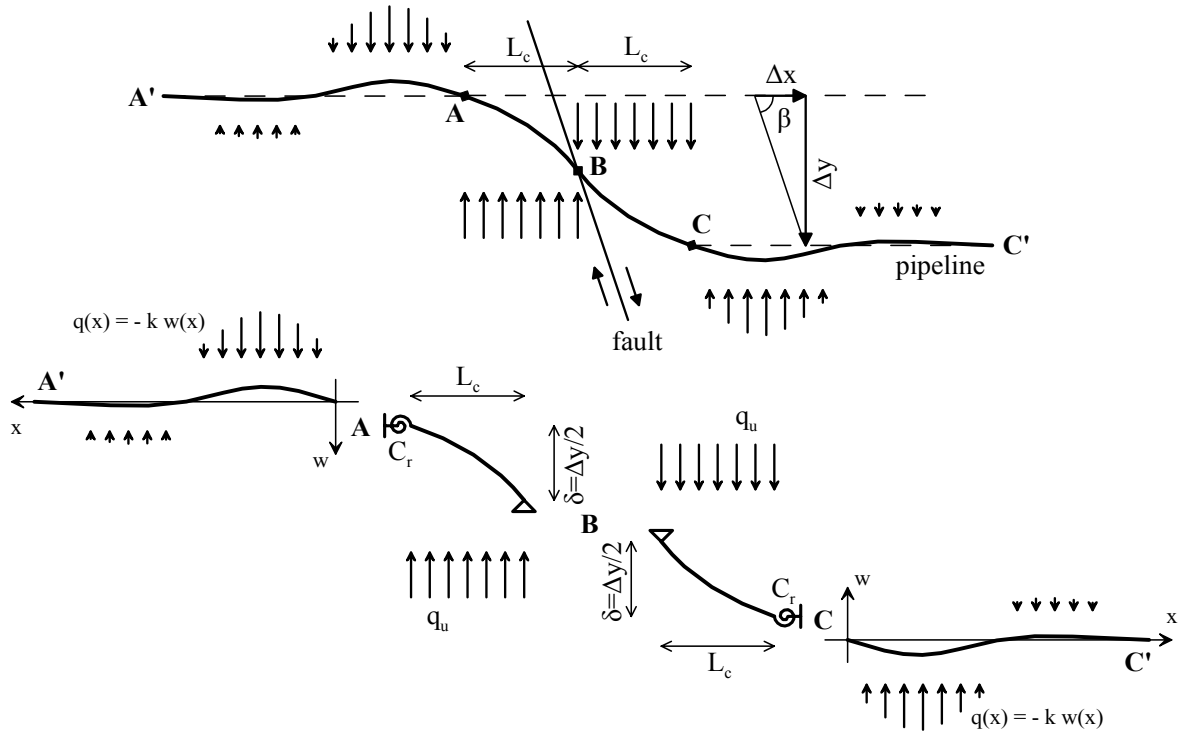

Figure 1. Partitioning of the pipeline into 4 segments

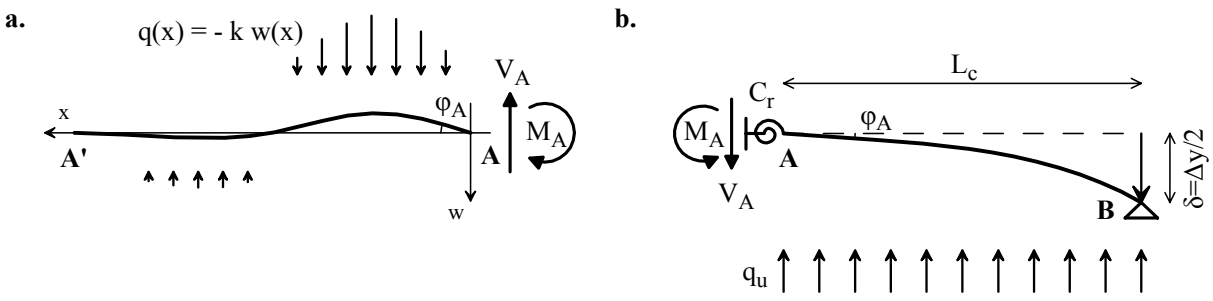

Figure 2. Analysis model for pipeline segments (a) AA´ (b) AB

The strike-slip fault is taken as an inclined plane, i.e. with null thickness of rupture zone, so that the intersection of the pipeline axis with the fault trace on the ground surface is reduced to a single point. The fault movement is defined in a Cartesian coordinate system, where the x-axis is collinear with the undeformed longitudinal axis of the pipeline, while the y-axis is perpendicular to x in the horizontal plane. Subsequently, the fault movement is analyzed into two Cartesian components, Δx and Δy, interrelated through the angle formed by the x-axis and the fault trace. In its present form, the proposed method applies to crossing angles $\beta \le 90°$, resulting in pipeline elongation.

Following the general concept originally introduced by Wang & Yeh (1985), the pipeline is partitioned into four (4) segments, defined by the characteristic points A, B and C in Figure 1: Point B is the intersection of the pipeline axis with the fault trace, while points A and C are the closest points of the pipeline axis with zero y displacement. The computation of combined axial and bending pipeline strains can be broken down into six (6) steps, briefly presented in the following. The detailed methodology workflow can be found in Karamitros et al. (2006), while a computer code for the application of the methodology can be downloaded from:
http://users.civil.ntua.gr/gbouck/en/publications.htm .

As in all similar design methodologies (Newmark and Hall, 1975, Kennedy et al., 1977, Wang and Yeh, 1985), the solution algorithm overlooks initial pipeline stresses due to soil overburden, as they are fairly small compared to the ones developing due to fault movement. Furthermore, pipeline and soil inertia effects are not taken into account as the velocity of the sliding part of the fault is considered to be sufficiently small, while concurrent spatially variable transient motion is neglected in the computations. Finally, it should be stressed that the proposed methodology overlooks local buckling and section deformation effects (Calladine, 1983), two phenomena which dominate pipeline behavior at large fault displacements. As a result, its application range is limited within the allowable strains which are explicitely defined by design codes (e.g. ALA-ASCE, 2005, CEN, 2003) in order to avoid such detrimental effects. For larger strain levels, rigorous numerical methods, or large displacement approximate methods (e.g. Takada et al., 2001) should be used.

Step 1
Segments AA′ and CC′ are analyzed as beams-on-elastic-foundation in order to obtain the relation between shear force, bending moment and rotation angle at points A and C. More specifically, setting $w = 0$ for $x = 0$ and $w \to 0$ for $x \to \infty$ in the differential equilibrium equation $E_1 I w'''' + kw = 0$ for the elastic line of segment AA′ (Figure 1), yields:

$$w = Ce^{-\lambda x} \sin \lambda x \tag{1a}$$

where:

$$\lambda = \sqrt[4]{\frac{k}{4E_1 I}} \tag{1b}$$

x is the distance from point A along the pipeline axis, w is the transverse horizontal displacement, E_1 is the elastic Young's modulus of the pipeline steel, I is the moment of inertia of the pipeline cross-section, and k is the constant of the transverse horizontal soil springs (Figure 2a). According to the ALA-ASCE (2005) guidelines, computation of k can be based on Hansen (1961) and Trautmann & O'Rourke (1983).

Differentiation of Eq. (1a) yields the following relations between the shear force $V_A = -E_1 I \cdot w'''_A$, the bending moment $M_A = -E_1 I \cdot w''_A$ and the rotation $\phi_A = w'_A$ at point A:

$$M_A = \left(2\lambda E_1 I\right) \cdot \phi_A \tag{2}$$

$$V_A = -\lambda \cdot M_A \tag{3}$$

Due to symmetry, similar relations apply for point C.

Step 2

Considering the boundary conditions determined in Step 1, segments AB and BC are analyzed with the elastic-beam theory, in order to derive the maximum bending moment M_{max}. Due to symmetry, the analysis can be focused on segment AB. This segment is modeled as an elastic beam, supported at point A by a rotational spring, whose constant is calculated from Eq. (2) as $C_r = 2\lambda E_l I$, and at point B by a joint, which is displaced by half the transverse component of the strike-slip fault movement, i.e. $\delta = \Delta y/2$. As a result, a uniformly distributed load q_u is applied to the beam, equal to the limit value of soil reaction for transverse horizontal movement of the pipeline relatively to the surrounding soil (Figure 2b). According to the ALA-ASCE (2005) guidelines, the value of q_u can be calculated from the properties of the backfill of the pipeline trench, based on the relations proposed by Hansen (1961) and Trautmann & O'Rourke (1983).

Application of the elastic-beam theory yields the following bending moment and shear force reactions on the supports A and B:

$$M_A = \frac{24EI\delta C_r - q_u C_r L_c^4}{24EIL_c + 8C_r L_c^2} \tag{4}$$

$$V_A = \frac{24EI\delta C_r - 12EIq_u L_c^3 - 5q_u C_r L_c^4}{24EIL_c^2 + 8C_r L_c^3} \tag{5}$$

$$V_B = \frac{24EI\delta C_r + 12EIq_u L_c^3 + 3q_u C_r L_c^4}{24EIL_c^2 + 8C_r L_c^3} \tag{6}$$

Eqs. (4)-(6) express the reaction forces of segments AB and BC in terms of the curved length L_c of the beam, which is not a priori known. However, substituting Eqs. (4) and (5) into Eq. (3) yields:

$$a_5 L_c^5 + a_4 L_c^4 + a_3 L_c^3 - a_1 L_c - a_0 = 0 \tag{7}$$

where a_0 to a_5 are known constants, equal to $a_0 = 24EI\delta C_r$, $a_1 = 24EI\delta C_r\lambda$, $a_3 = 12EIq_u$, $a_4 = 5q_u C_r$ and $a_5 = q_u C_r \lambda$.

The above polynomial equation can be solved iteratively, using the Newton-Raphson method, with a large initial value for L_c (e.g. 500m). In this way, the values of M_A, V_A, and V_B can be directly estimated, and the maximum bending moment developing on the pipeline can be consequently calculated from the elastic-beam theory, as:

$$M_{max} = \frac{3V_B^{\,2}}{2q_u} x_{max} \tag{8}$$

Step 3

Similar to all existing methodologies (Newmark and Hall, 1975, Kennedy et al., 1977, Wang and Yeh, 1985), the axial force at the intersection of the pipeline with the fault trace is calculated from the requirement for compatibility between the geometrically required and the stress-induced (available)

pipeline elongation. The required elongation ΔL_{req} is defined as the elongation imposed to the pipeline due to the fault movement. For the sake of simplicity, the elongation provoked by the Δy fault displacement component may be neglected, as it is minimal compared to the elongation due to the Δx component. Therefore:

$$\Delta L_{req} \approx \Delta x \tag{9}$$

On the other hand, the available elongation ΔL_{av} is defined as the elongation resulting from the integration of axial strains along the unanchored length, i.e. the length over which slippage occurs between the pipeline and the surrounding soil:

$$\Delta L_{av} = 2 \int_{0}^{Lanch} \varepsilon(L) \cdot dL \tag{10}$$

where L is the distance from the fault trace, while the factor 2, by which the integral in Eq. (10) is multiplied, accounts for the elongation on both sides of the fault trace.

The unanchored length L_{anch} may be calculated from the equilibrium along the pipeline axis, assuming that axial pipeline stresses essentially become zero at the far end of the unanchored length. In this way, L_{anch} is expressed as:

$$L_{anch} = \frac{F_a}{t_u} = \frac{\sigma_a A_s}{t_u} \tag{11}$$

where F_a and σ_a are the axial force and stress developing in the intersection of the pipeline axis with the fault trace, A_s is the area of the pipeline cross-section and t_u is the limit friction due to the slippage of the pipeline relatively to the surrounding soil (ALA-ASCE, 2005).

The distribution of strains along the unanchored length can be consequently derived from the corresponding stresses, assuming a bilinear stress-strain relationship for the pipeline steel. Assuming further that axial stresses attenuate linearly with the distance from the fault trace, due to the constant value of the limit friction force, tensile stresses along the pipeline axis can be expressed as:

$$\sigma(L) = \sigma_a - \frac{t_u}{A_s} L \tag{12}$$

For the case where the axial tensile stress σ_a is below the yield limit σ_1, Eq. (10) can be re-written as:

$$\Delta L_{av} = 2 \int_{0}^{Lanch} \frac{\sigma(L)}{E_1} \cdot dL = \frac{\sigma_a^2 A_s}{E_1 t_u} \tag{13}$$

Therefore, for $\Delta L_{av} = \Delta L_{req}$, the maximum tensile stress becomes:

$$\sigma_a = \sqrt{\frac{E_1 t_u \Delta L_{req}}{A_s}} \tag{14}$$

If the required elongation is larger than the one corresponding to $\sigma_a = \sigma_1$, i.e. when:

$$\Delta L_{req} > \frac{\sigma_1^{\,2} A_s}{E_1 t_u} \tag{15}$$

then plastic strains develop in the pipeline and Eq. (10) becomes:

$$\Delta L_{av} = 2\left[\int_0^{L_1}\left(\varepsilon_1 + \frac{\sigma(L)-\sigma_1}{E_2}\right)\cdot dL + \int_{L_1}^{Lanch}\frac{\sigma(L)}{E_1}\cdot dL\right] \tag{16}$$

where:

$$L_1 = \frac{(\sigma_a - \sigma_1)A_s}{t_u} \tag{17}$$

Combining Eq. (11), (12), (16) and (17), the maximum developing tensile stress becomes:

$$\sigma_a = \frac{\sigma_1(E_1 - E_2) + \sqrt{\sigma_1^2\left(E_2^2 - E_1E_2\right) + E_1^2E_2\Delta L_{req}\dfrac{t_u}{A_s}}}{E_1} \tag{18}$$

Regardless of the axial stress level, the corresponding axial force is equal to:

$$F_a = \sigma_a A_s \tag{19}$$

Step 4
According to the elastic beam theory, bending strains on the pipeline can be calculated as:

$$\varepsilon_b^{I} = \frac{M_{max}D}{2EI} \tag{20}$$

where D is the external pipeline diameter.

The above equation is accurate for small fault displacements, while for larger fault displacements, geometrical second-order effects must be also taken into account. To simplify this relatively complex problem, the bending stiffness of the pipeline may be approximately neglected (Kennedy et al., 1977), so that bending strains can be computed geometrically as:

$$\varepsilon_b^{II} = \frac{D/2}{R} \tag{21}$$

The radius of curvature R results from the equilibrium of the forces acting on an infinitesimal part of the pipeline's curved length:

$$R = \frac{F_a}{q_u} \tag{22}$$

and finally:

$$\varepsilon_b^{II} = \frac{q_u D}{2F_a} \tag{23}$$

Eq. (23) indicates that bending strains induced by second-order effects are inversely proportional to the axial force applied on the pipeline. In other words, for small fault displacements, bending strains computed by Eq. (23) tend to become infinite. This is due to the fact that Eq. (22) has been derived assuming that the pipeline bending stiffness is equal to zero, which is approximately true only when the whole pipeline cross-section is under yield.

According to the above, the actual bending strain ε_b lays between ε_b^I and ε_b^{II}, asymptotically approaching ε_b^I as fault displacements tend to zero and ε_b^{II} in the opposite case. Here, it is approximately assumed that:

$$\frac{1}{\varepsilon_b} = \frac{1}{\varepsilon_b^I} + \frac{1}{\varepsilon_b^{II}} \tag{24}$$

Step 5

Existing methodologies (Newmark and Hall, 1975, Kennedy et al., 1977, Wang and Yeh, 1985) calculate the axial strain directly from the axial stress, using the adopted stress-strain relation for the pipeline steel. When strains in the pipeline cross-section remain in the elastic range, this assumption is valid for every point along the pipeline axis. However, when yielding occurs, it is accurate only at the intersection of the pipeline with the fault trace, where the bending strain is zero. In the vicinity of the cross-section where the maximum bending strain occurs, axial strain increases locally, so that the integral of stresses on the pipeline cross-section remains equal to the applied axial force.

In the present work, the interaction between axial and bending strains is quantified by determining the exact distribution of strains and stresses on the pipeline cross-section. For this purpose, the beam-theory assumption of plane cross-sections is embraced, while the stress-strain curve of the pipeline steel is considered to be bilinear.

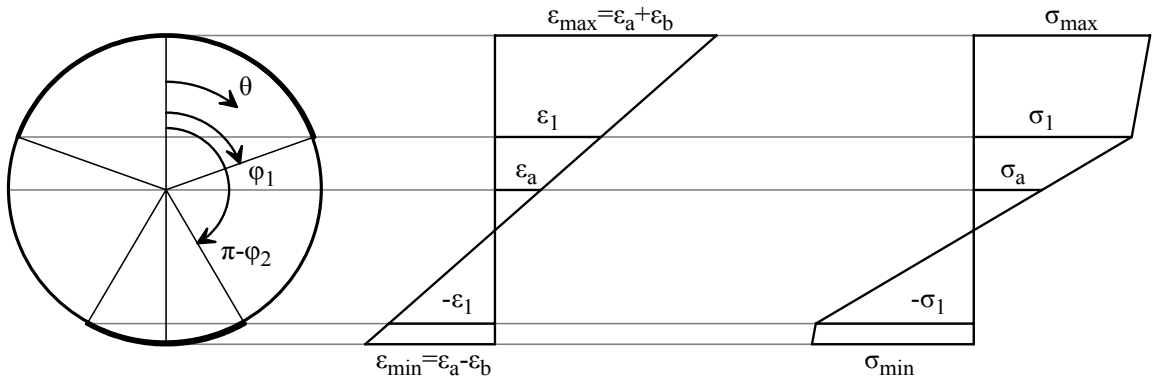

Figure 3. Non-linear stress and strain distribution on the pipeline cross-section

Bearing in mind the above, the strain distribution on the cross-section is given by Eq. (25):

$$\varepsilon = \varepsilon_a + \varepsilon_b \cos\theta \tag{25}$$

where the angle θ is the polar angle of the cross-section, defined in Figure 3. The corresponding distribution of stresses on the pipeline cross-section is given by Eq. (26):

$$\sigma = \begin{cases} \sigma_1 + E_2(\varepsilon - \varepsilon_1) & 0 \le \theta < \phi_1 \\ E_1\varepsilon & \phi_1 \le \theta \le \pi - \phi_2 \\ -\sigma_1 + E_2(\varepsilon + \varepsilon_1) & \pi - \phi_2 < \theta \le \pi \end{cases} \tag{26}$$

where the angles $\varphi_{1,2}$ define the portion of the cross-section that is under yield (Figure 3), and are calculated as:

$$\phi_{1,2} = \begin{cases} \pi & \dfrac{\varepsilon_1 \mp \varepsilon_a}{\varepsilon_b} < -1 \\ \arccos\left(\dfrac{\varepsilon_1 \mp \varepsilon_a}{\varepsilon_b}\right) & -1 \le \dfrac{\varepsilon_1 \mp \varepsilon_a}{\varepsilon_b} \le 1 \\ 0 & 1 < \dfrac{\varepsilon_1 \mp \varepsilon_a}{\varepsilon_b} \end{cases} \tag{27}$$

The total axial force is calculated by integrating the stresses over the cross-section, as:

$$\begin{aligned} &F = 2\int_0^{\pi} \sigma R_m t d\theta \Rightarrow \\ &F = 2R_m t \cdot \left[\begin{aligned} &E_1 \pi \varepsilon_a - (E_1 - E_2)(\phi_1 + \phi_2)\varepsilon_a + \\ &(E_1 - E_2)(\phi_1 - \phi_2)\varepsilon_1 - (E_1 - E_2)(\sin\phi_1 - \sin\phi_2)\varepsilon_b \end{aligned} \right] \end{aligned} \tag{28}$$

where:

$$R_m = \frac{D - t}{2} \tag{29}$$

The axial strain of the pipeline can be derived from the demand for equilibrium, by equating the axial force computed using Eq. (28), to the one calculated using Eq. (19). Note that Eq. (19) applies strictly at the pipeline's intersection with the fault trace, but it is approximately extended to the neighboring position of the maximum bending moment. The solution of the system of Eqs. (27) and (28) results in a complex formula for ε_a, which can be solved iteratively, using the Newton-Raphson method and starting from an initial value of $\varepsilon_a^0 = 0$.

Having calculated the axial strain at the position of maximum bending strain, the minimum and maximum longitudinal strains can be subsequently computed as their algebraic sum (i.e. $\varepsilon_{max,min} = \varepsilon_a \pm \varepsilon_b$).

Step 6

The analysis of segments AB and BC, from which the maximum bending moment emerges, is based on the elastic beam theory and is not taking into account the non-linear behavior of the pipeline steel. Since the steel stress-strain relationship is considered to be bilinear, a series of equivalent linear calculation loops is performed, employing a procedure for readjusting the secant Young's modulus of the pipeline steel on each loop.

More specifically, using the already defined stress distribution on the pipeline cross-section, the corresponding bending moment can be calculated using Eq. (30):

$$M = 2\int_0^{\pi} \sigma R_m t R_m \cos\theta d\theta \Rightarrow$$

$$M = 2R_m{}^2 t \cdot \left[\begin{array}{l} \dfrac{E_1 \pi \varepsilon_b}{2} - (E_1 - E_2)(\sin\phi_1 - \sin\phi_2)\varepsilon_a + (E_1 - E_2)(\sin\phi_1 + \sin\phi_2)\varepsilon_1 \\ -\dfrac{(E_1 - E_2)(\phi_1 + \phi_2)\varepsilon_b}{2} - \dfrac{(E_1 - E_2)(\sin 2\phi_1 + \sin 2\phi_2)\varepsilon_b}{4} \end{array} \right] \quad (30)$$

Therefore, the secant modulus for the next iteration can be calculated as:

$$E'_{sec} = \frac{M(\varepsilon_a, \varepsilon_b) \cdot D}{2I\varepsilon_b^I} = \frac{M(\varepsilon_a, \varepsilon_b) \cdot D}{2I}\left(\frac{1}{\varepsilon_b} - \frac{1}{\varepsilon_b^{II}}\right) \quad (31)$$

and Steps 2 to 6 are repeated, until convergence is accomplished.

VALIDATION OF THE PROPOSED METHODOLOGY

To validate the results of the proposed methodology, analytical predictions are compared to the results from a series of 3-D non-linear numerical analyses with the Finite Element Method, performed with the commercial code MSC/NASTRAN (The MacNeal – Schwendler Corporation, 1994). For this purpose, a typical high-pressure natural gas pipeline was considered, featuring an external diameter of 0.9144m (36in), a wall thickness of 0.0119m (0.469in), and a total length of 1000m. A hybrid model was used for the simulation of the pipeline, with a part of 50m along both sides of the fault trace (i.e. a total length of 100m) modeled as a cylindrical shell, and the remaining 450m part (i.e. a total length of 900m) modeled as a beam (Figure 4). The shell perimeter was discretized into 16 equal sized quadrilateral shell elements, each of 0.20m length. The beam part was discretized with 0.50m long beam elements. The pipeline steel was of the API5L-X65 type, with a bilinear elasto-plastic stress-strain curve and the properties listed in Table 1.

To simulate soil-pipeline interaction effects, each node of the model was connected to axial, transverse horizontal and vertical soil springs, modeled as elastic-perfectly plastic rod elements. The properties of the soil-springs (Table 3) were calculated according to the ALA-ASCE (2005) guidelines, assuming that the pipeline top is buried under 1.30m of medium-density sand with friction angle φ=36º and unit weight γ=18kN/m^2. The fault movement was applied statically at the sliding part of the fault, as a permanent displacement of the free end of the corresponding soil-springs.

Table 1: API5L-X65 steel properties considered in the numerical analyses

Yield stress (σ_1)	490MPa
Failure stress (σ_2)	531MPa
Failure strain (ε_2)	4.0%
Elastic Young's modulus (E_1)	210GPa
Yield strain ($\varepsilon_1 = \sigma_1 / E_1$)	0.233%
Plastic Young's modulus ($E_2 = (\sigma_2 - \sigma_1)/(\varepsilon_2 - \varepsilon_1)$)	1.088GPa

Table 2: Soil spring properties considered in the numerical analyses

	Yield force	Yield displacement
Axial (friction) springs	40.5 kN/m	3.0 mm
Transverse horizontal springs	318.6 kN/m	11.4 mm
Vertical springs (upward movement)	52.0 kN/m	2.2 mm
Vertical springs (downward movement)	1360.0 kN/m	100.0 mm

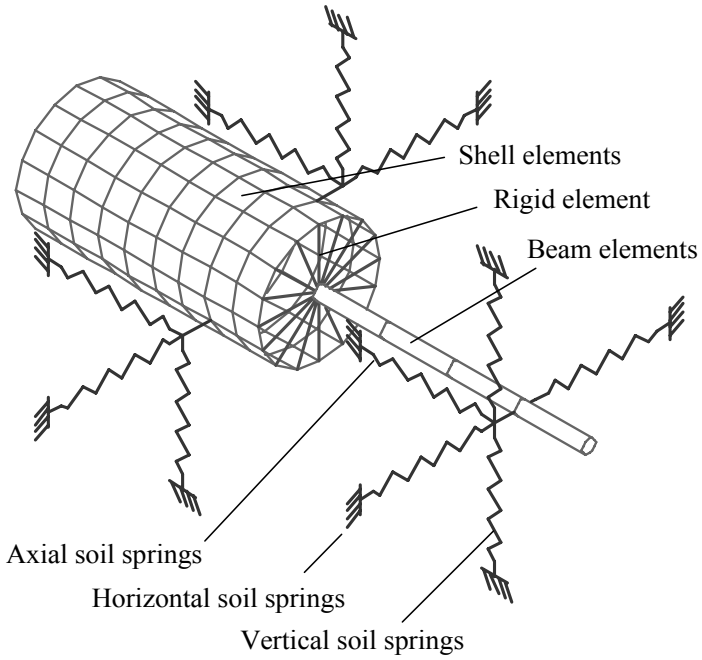

Figure 4. 3-D model used for analyses with the Finite Element Method: the junction between shell and beam part

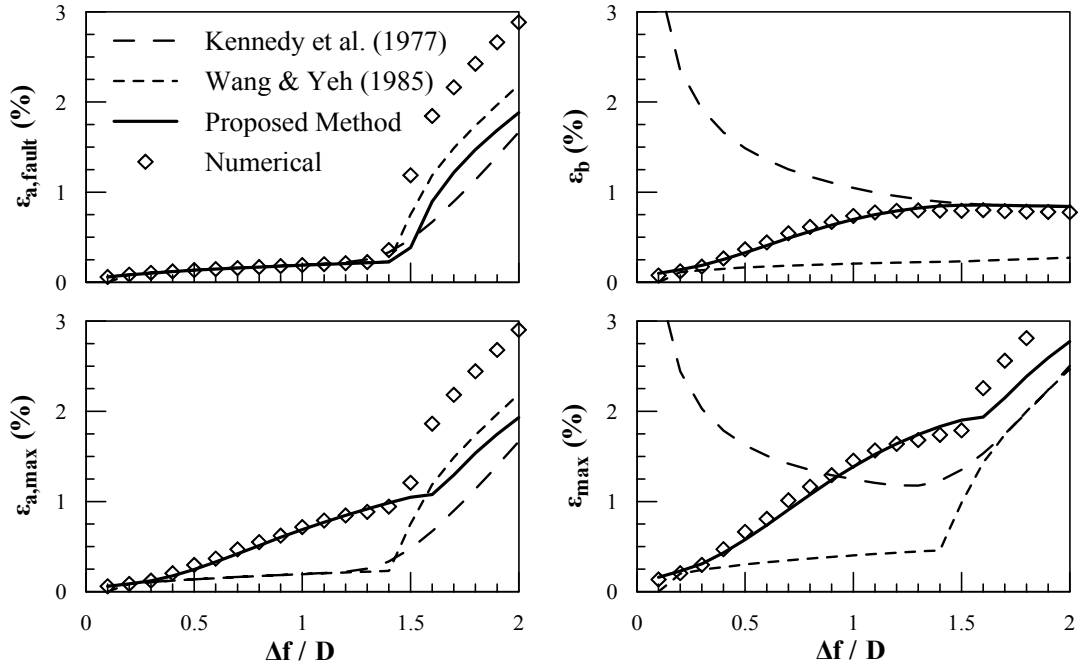

Figure 5. Comparison of the results of the proposed analytical methodology with the results of the numerical analyses and the predictions of the Kennedy et al. (1977) and Wang & Yeh (1985) methods

Considering the intersection angle between the fault trace and the pipeline axis to be equal to $\beta = 45^{\circ}$, the analysis proceeded incrementally to a final fault displacement $\Delta f = 2D$. Results from analyses for different angles β are presented in Karamitros et al. (2006).

The numerical results are presented in Figure 5 in comparison with analytical predictions according to the proposed methodology, as well as the methodologies of Kennedy et al. (1977) and Wang & Yeh (1985). The top left graph of Figure 5 shows the comparison between analytical and numerical

predictions of axial strain $\varepsilon_{a,fault}$ at the pipeline-fault trace intersection. The agreement appears fairly good, for all analytical methods. As the main assumption for computing $\varepsilon_{a,fault}$ is the compatibility between the geometrically required and the stress induced (available) elongation of the pipeline, the observed agreement is essentially considered as a solid verification of this assumption.

The bottom left graph of Figure 5 refers to the overall maximum axial strain $\varepsilon_{a,max}$, which does not necessarily develop at the pipeline-fault trace intersection, as the existing analytical methods imply. In this case, a good overall agreement is observed only between numerical results and analytical predictions with the proposed methodology. The existing analytical methods approach the numerical solution at large displacements, after the yield strain of the pipeline steel has been exceeded, while they grossly under-predict $\varepsilon_{a,max}$ at smaller displacements. Note that observed differences are larger at intermediate displacement levels, of the order of $\Delta f \approx 1D$, which are commonly encountered in practice.

Focusing next on bending strains ε_b (top right graph of Figure 5), a good overall agreement is observed again between the proposed analytical method and the numerical analyses. The Kennedy et al. (1977) method proves accurate in the region of large displacements ($\Delta f/D > 1.5$), i.e. when the criteria for the applicability of the method are met, but seriously over-predicts ε_b for smaller fault displacements. The Wang & Yeh (1985) method under-predicts ε_b for the entire range of fault displacements analyzed herein, mainly because it neglects the effect of axial tension on the pipeline bending stiffness.

The maximum longitudinal strains $\varepsilon_{max} = \varepsilon_{a,max} + \varepsilon_b$ are probably the best criterion for the evaluation of the proposed methodology, as they form the basis of pipeline design. From the bottom right graph of Figure 5, it may be observed that the good overall performance of the proposed method, acknowledged in the previous comparisons, applies here as well. As expected, the Kennedy et al. (1977) method over-predicts maximum strains for small fault displacements. This trend is reversed at intermediate levels of fault displacement, and the divergence is gradually reduced as displacements increase. Finally, the methodology of Wang & Yeh (1985) provides accurate results only in the region of large displacements, where axial tension is the prevailing mode of deformation. For small and intermediate fault displacements ε_{max} is consistently under-estimated.

CONCLUSION

An improved analytical methodology has been developed for the stress analysis of buried steel pipelines crossing active strike-slip faults. It is based on firm assumptions adopted in the existing analytical methodologies of Kennedy et al. (1977) and Wang & Yeh (1985), but proceeds further:

- to analyze the curved part of the pipeline with the aid of elastic-beam theory, in order to locate the most unfavorable combination of axial and bending strains, and
- to consider the actual stress distribution on the pipeline cross-section, in order to account for the effect of curvature on axial strains and calculate the design maximum strain.

Acknowledging that there is no end to the refinements that can be applied to simplified analytical methodologies, it needs to be stressed out that the above modifications considerably improve the accuracy of analytical predictions, especially for small and medium fault displacements, while they still permit a simple analytical solution algorithm to be developed. In fact, although more complicated than the most commonly used today method of Kennedy et al. (1977), the computational algorithm of the proposed methodology remains relatively simple and stable, and can be easily programmed for quick application.

Note that, in its present form, the proposed method applies to intersection angles $\beta \leq 90°$ resulting in elongation of the pipeline. Furthermore, it does not account for the effects of local buckling and section deformation. Therefore, its application should not be extended beyond the strain limits explicitely defined by design codes in order to mitigate such phenomena.

ACKNOWLEDGEMENTS

This research is supported by the "EPEAEK II Pythagoras" grant, co-funded by the European Social Fund (75%) and the Hellenic Ministry of Education (25%).

REFERENCES

American Lifelines Alliance – ASCE. Guidelines for the Design of Buried Steel Pipe, July 2001 (with addenda through February 2005).

ASCE Technical Council on Lifeline Earthquake Engineering. Differential Ground Movement Effects on Buried Pipelines. Guidelines for the Seismic Design of Oil and Gas Pipeline Systems, 150-228, 1984.

Calladine CR. Theory of Shell Structures, Cambridge, Cambridge University Press, 1983.

CEN European Committee for Standardisation. Eurocode 8: Design of structures for earthquake resistance, Part 4: Silos, tanks and pipelines, Draft No 2, Ref. No. EN1998-4: 2003 (E), December 2003.

EERI. The Izmit (Kocaeli), Turkey Earthquake of August 17, 1999. EERI Special Earthquake Report, 1999.

Hansen JB. The Ultimate Resistance of Rigid Piles Against Transversal Forces. Bulletin 12. Danish Geotechnical Institute, Copenhagen, Denmark, 1961.

Karamitros DK, Bouckovalas GD, and Kouretzis GP. "Stress analysis of buried steel pipelines at strike-slip fault crossings," Soil dynamics and Earthquake Engineering, doi:10.1016/ j.soildyn.2006.08.001, 2006.

Kennedy RP, Chow AW, and Williamson RA. "Fault Movement Effects on Buried Oil Pipeline," Transportation Engineering Journal, ASCE, 103, 617-633, 1977.

Newmark NM and Hall WJ. "Pipeline Design to Resist Large Fault Displacement," Proceedings of the U.S. National Conference on Earthquake Engineering. Ann Arbor, University of Michigan, 416-425, 1975.

Takada S, Hassani N, and Fukuda K. "A New Proposal for Simplified Design of Buried Steel Pipes Crossing Active Faults," Earthquake Engineering and Structural Dynamics, 30, 1243-1257, 2001.

The MacNeal - Schwendler Corporation. MSC/NASTRAN for Windows: Reference Manual, 1994.

Trautmann CH and O'Rourke TD. Behavior of Pipe in Dry Sand Under Lateral and Uplift Loading. Geotechnical Engineering Report 83-6. Cornell University, Ithaca, New York, 1983.

Uzarski J and Arnold C. "Chi-Chi, Taiwan, Earthquake of September 21, 1999, Reconnaissance Report," Earthquake Spectra, The Professional Journal of the EERI, 17(Supplement A), 2001.

Wang LRL and Yeh Y. "A Refined Seismic Analysis and Design of Buried Pipeline for Fault Movement," Earthquake Engineering and Structural Dynamics, 13, 75-96, 1985.